Protein Science (1999), *8*:2444–2454. Cambridge University Press. Printed in the USA.

Conformational and metal-binding properties of androcam, a testis-specific, calmodulin-related protein from *Drosophila*

STEPHEN R. MARTIN,[1] ALAN Q. LU,[2] JIE XIAO,[2] JENS KLEINJUNG,[1]
KATHY BECKINGHAM,[2] AND PETER M. BAYLEY[1]

[1]Division of Physical Biochemistry, National Institute for Medical Research, The Ridgeway, Mill Hill, London NW7 1AA, United Kingdom
[2]Department of Biochemistry and Cell Biology, MS 140, Rice University, 6100 Main St., Houston, Texas 77005-1892

(RECEIVED June 15, 1999; ACCEPTED August 13, 1999)

Abstract

Androcam is a testis-specific protein of *Drosophila melanogaster*, with 67% sequence identity to calmodulin and four potential EF-hand calcium-binding sites. Spectroscopic monitoring of the thermal unfolding of recombinant calcium-free androcam shows a biphasic process characteristic of a two-domain protein, with the apo-N-domain less stable than the apo-C-domain. The two EF hands of the C-domain of androcam bind calcium cooperatively with 40-fold higher average affinity than the corresponding calmodulin sites. Magnesium competes with calcium binding [K_a(Mg) $\sim 3 \times 10^3$ M^{-1}]. Weak calcium binding is also detected at one or more N-domain sites. Compared to apo-calmodulin, apo-androcam has a smaller conformational response to calcium and a lower α-helical content over a range of experimental conditions. Unlike calmodulin, a tryptic cleavage site in the N-domain of apo-androcam remains trypsin sensitive in the presence of calcium, suggesting an altered calcium-dependent conformational change in this domain. The affinity of model target peptides for androcam is 10^3–10^5 times lower than for calmodulin, and interaction of the N-domain of androcam with these peptides is significantly reduced. Thus, androcam shows calcium-induced conformational responses typical of a calcium sensor, but its properties indicate calcium sensitivity and target interactions significantly different from those of calmodulin. From the sequence differences and the altered calcium-binding properties it is likely that androcam differs from calmodulin in the conformation of residues in the second calcium-binding loop. Molecular modeling supports the deduction that there are significant conformational differences in the N-domain of androcam compared to calmodulin, and that these could affect the surface, conferring a different specificity on androcam in target interactions related to testis-specific calcium signaling functions.

Keywords: calcium binding; calmodulin; modeling; spectroscopy, stability, testis

The calcium-signaling protein calmodulin (CaM) has been remarkably conserved in evolution. For example, CaM proteins from mammalian (bovine) and arthropod (*Drosophila*) species show 98% sequence identity (see Cohen & Klee, 1988, for reviews). In most animals, a single version of CaM is present and expressed ubiquitously throughout the organism. However, CaM-related proteins with more limited expression patterns are being identified across all evolutionary orders (e.g., Yaswen et al., 1992; Andres & Thummel, 1995), suggesting the continuous evolution of more specialized molecules adapted to specific calcium-related functions. The muscle-specific troponin C proteins, which typically show 40–50% sequence identity to CaM, perhaps best exemplify this more specialized class of calcium-signaling-related proteins.

In investigating CaM-related genes in *Drosophila melanogaster*, we detected a single cross-hybridizing gene (Doyle et al., 1990) that was subsequently shown to encode a protein with 67% sequence identity to CaM (Fyrberg et al., 1994) (Fig. 1). Like CaM, this protein contains four "EF-hand"–type sequences (Kretsinger, 1980), which could potentially bind calcium. Recently we have established that this *Drosophila* protein is a tissue-specific gene product, uniquely expressed in the male gonad. Given this testis-specific expression, we have termed the gene/protein androcam (Acam) (Lu & Beckingham, 1997). Immunolocalization studies have demonstrated that Acam is present throughout most stages of

Reprint requests to: Peter M. Bayley, Division of Physical Biochemistry, National Institute for Medical Research, The Ridgeway, Mill Hill, London NW7 1AA, United Kingdom; e-mail: p-bayley@nimr.mrc.ac.uk.

Abbreviations: Acam, *Drosophila melanogaster* androcam; CaM, *D. melanogaster* calmodulin; CD, circular dichroism; DTT, dithiothreitol; EGTA, ethylene-glycol-bis(β-aminoethyl ether)-*N,N,N′,N′*-tetracetic acid; holo-CaM and holo-Acam, calcium-saturated forms of CaM and Acam, respectively; HSQC, heteronuclear single quantum coherence; IPTG, isopropyl-β-D-thiogalactopyranoside; Mg-Acam, magnesium-saturated Acam; sk-MLCK, skeletal myosin light-chain kinase; UV, ultraviolet.

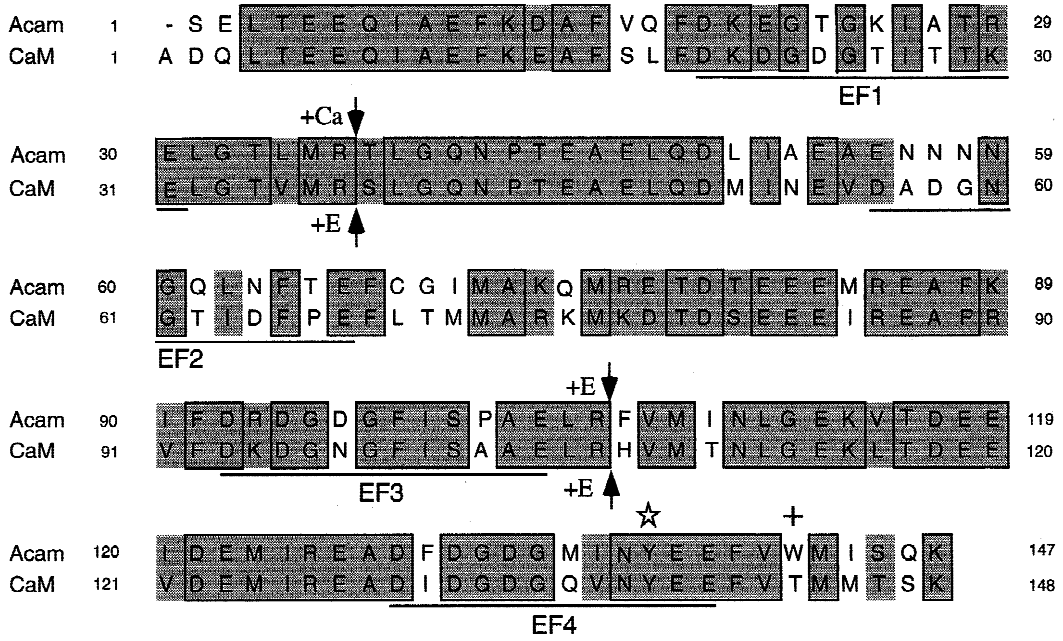

Fig. 1. Alignment of Acam and *Drosophila* CaM protein sequences. The Acam amino acid sequence is from Fyrberg et al. (1994), with the I-L correction at residue 104 incorporated (see Materials and methods). The *Drosophila* CaM sequence is from Smith et al. (1987). Acam is 67% identical and 85% similar to *Drosophila* CaM. Identical residues are boxed and shaded; conservative changes are shaded. Calcium-binding loops of EF hands 1, 2, 3, and 4 of CaM are marked. ☆, Single tyrosine residue of both Acam and CaM; +, single tryptophan present uniquely in Acam. Primary trypsin cleavage sites in the presence of EDTA (+E) or calcium (+Ca) for each protein are indicated by short arrows.

spermatogenesis showing a dynamic pattern of subcellular localization as gametogenesis proceeds. Early in spermatogenesis, Acam is predominantly nuclear and is bound to the "lampbrush-like" loops of the Y chromosome; later, Acam is diffusely localized throughout the elongating sperm tail and remains present in mature sperm detected in the female reproductive tract (A.Q. Lu & K. Beckingham, unpubl. obs.).

These unusual properties suggest that Acam is involved in calcium-related events specific to spermatogenesis and mature sperm function. We have, therefore, generated and purified bacterially expressed Acam, determined its calcium-binding properties, and examined calcium-induced conformational changes, using many of the biophysical parameters previously employed to characterize CaM. The unique tryptophan of Acam and the single tyrosine in the fourth EF hand of Acam (cf. *Drosophila* CaM; see Fig. 1) proved to be valuable spectroscopic probes for monitoring conformational changes in this region of the protein.

Our findings indicate that Acam, like CaM itself, has the potential to be a calcium-signal transducer protein because it undergoes significant conformational changes upon calcium binding. However, our results also suggest that Acam has roles distinct from those of CaM. Thus, Acam is predicted to respond to a different range of intracellular calcium concentrations, to adopt a detectably different calcium-bound conformation, and to possess target interaction properties that differ from those of CaM.

Results

Purification of recombinant Acam

Construction of the vector used for bacterial expression of Acam is described in Materials and methods. Purification of Acam from the bacterial lysates was initially attempted using phenyl-sepharose affinity chromatography at low ionic strength (50 mM NaCl, as used for CaM). However, Acam showed poor binding and continuous leaching from the resin under these conditions. Inclusion of 500 mM NaCl in the binding buffer and column washes gave quantitative retention of the protein and permitted complete purification in high yield. The phenyl-sepharose binding properties of Acam are strikingly similar to those of a series of CaM mutants, in each of which a single calcium-binding site was inactivated (Maune et al., 1992b). This similarity suggests that, as for these CaM mutants, the calcium-induced conformational change in Acam yields a protein with less surface hydrophobicity than CaM itself. Nevertheless, as for CaM, the holo-form of Acam shows a substantial mobility shift relative to the apo-form on SDS-PAGE electrophoresis (Fig. 2A). As for CaM, this mobility shift was not seen when magnesium was substituted for calcium.

Trypsin sensitivity of Acam

CaM is rapidly digested by trypsin in the absence of calcium at 2 of the 10 potential trypsin cleavage sites. The major cleavage is at Arg106 in the C-terminal lobe (Walsh et al., 1977). A low level of cleavage is also seen at Arg37 in the N-terminus, although scission at both sites in a single molecule is not detected (Kawasaki et al., 1986; Mackall & Klee, 1991). Upon calcium binding, these trypsin-sensitive bonds become resistant to digestion such that Arg74, Lys75, and Lys77 in the central flexible linker region are the major initial cleavage sites in holo-CaM (Walsh et al., 1977; Kawasaki et al., 1986). Two major fragments representing the N- and C-terminal lobes are thus initially produced. Interestingly, cleavage rate studies indicate that the absolute rates of scission at Arg74, Lys75, and Lys77 in the absence or presence of high calcium are

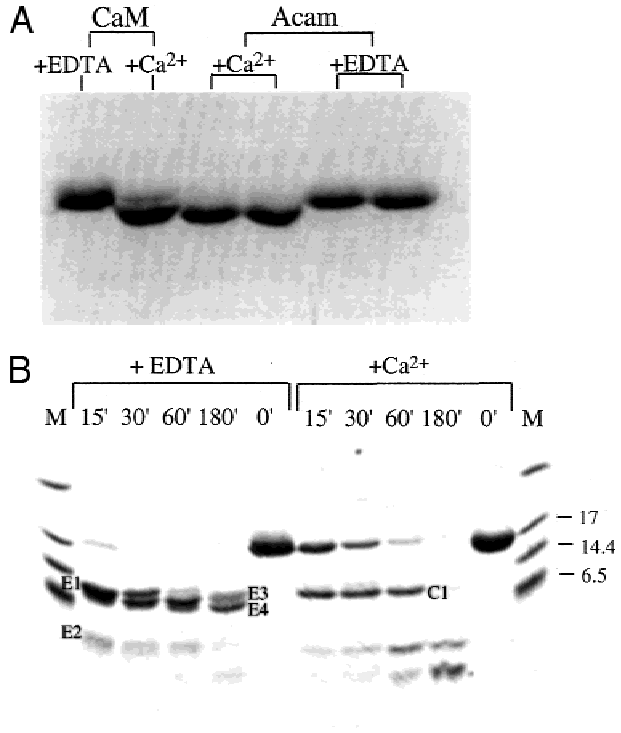

Fig. 2. A: Calcium-dependent mobility shifts in Acam and CaM. Bacterially expressed and purified Acam and *Drosophila* CaM (10 μg aliquots) after SDS-PAGE on a 12.5% gel. Sample buffer contained 5 mM $CaCl_2$ ($+Ca^{2+}$) or 5 mM EDTA (+EDTA). **B:** Trypsin digestion of Acam in the presence of EDTA or calcium. Aliquots of Acam (10 μg) were digested with trypsin at a 1:500 enzyme:substrate ratio in the presence of 1 mM $CaCl_2$ or 1 mM EDTA. Peptides present after 0–180′ of digestion are shown. Sizes of standards (KD) in molecular weight marker lanes (M) are indicated. N-Terminal sequencing was performed for peptides E1, E2, E3, and C1 (see text).

comparable, their prominence in the presence of high calcium thus reflecting the protection of Arg37 and Arg106 from cleavage (Mackall & Klee, 1991). This pattern of digestion corroborates the overall view of the conformational change in CaM that has emerged from many studies, including ones described herein: the C-terminal lobe appears the most readily digestible part of the protein in the absence of calcium, but calcium binding converts both lobes into highly ordered, trypsin-resistant structures.

Like CaM, Acam proved more trypsin sensitive in the absence of calcium, yielding as initial cleavage products, peptides E1 and E2 of apparent molecular weights 11 and 4 kDa (Fig. 2B). N-terminal sequencing established that these peptides represent products of cleavage at Arg105 (corresponding to Arg106 in CaM, Fig. 1). Thus, in the absence of calcium, Acam shows an identical initial cleavage pattern to CaM. After the initial cleavage, peptide 1–105 of Acam is progressively digested at two further positions to yield two fragments (E3, E4) running in close proximity to peptide E1. N-terminal sequencing of the first of these two fragments to be generated (E3) established that it results from cleavage of peptide E1 (1–105) in its C-terminal region. Again this is very reminiscent of apo-CaM for which the 1–106 peptide undergoes secondary cleavage at Arg90 (Walsh et al., 1977; Kawasaki et al., 1986). Arg90 is conserved in Acam (Arg89) and, thus, this secondary cleavage event may also be conserved. The nature of the third peptide (E3) was not investigated.

In contrast, the Acam peptide pattern produced in the presence of calcium differed markedly from that of CaM. N-terminal sequencing of the single large peptide, C1, produced by primary cleavage (apparent molecular weight 11 kDa, see Fig. 2B) established that this reflected cleavage at Arg36 (equivalent to Arg37 in CaM, Fig. 1). As noted above, this is the minor cleavage site for trypsin in the N-terminus of apo-CaM, which becomes resistant at high calcium levels. Acam digestion in the presence of 1, 10, and 20 mM $CaCl_2$ yielded identical cleavage patterns although digestion was somewhat slower at high calcium levels.

The persistence of this Arg36 tryptic cleavage site in Acam even in the presence of high calcium suggests a loss of calcium binding affinity at one or both N-terminal EF-hands of the protein. The absence of detectable cleavage of Acam at sites comparable to Arg74, Lys75, and Lys77 of CaM in the presence of calcium could reflect real protection of these sites in holo-Acam, or may simply be a consequence of the retention of the Arg36 cleavage point. As indicated above, the detection of cleavage at Arg74, Lys75, and Lys77 in holo-CaM does not reflect heightened sensitivity of these peptide bonds upon calcium binding, but rather the loss of scission at the preferred Arg37 and Arg106 sites.

Calcium binding

Calcium titrations of apo-Acam in the presence of 5,5′-Br_2BAPTA or Quin2 were used to measure stoichiometric calcium association constants (Table 1). In practice, these indicators are able to report association constants in the range 5×10^8 to 1×10^4 M^{-1}. Typical curves are shown in Figure 3. The value of K_3 for Acam is close to the lower limit measurable with 5,5′-Br_2BAPTA and is, therefore, poorly determined; incorporating K_4 (in addition to K_3) as a variable gives no significant improvement in the fit. The numerical

Table 1. *Stoichiometric Ca^{2+}-binding constants for CaM and Acam*[a]

Protein	$\log(K_1)$	$\log(K_2)$	$\log(K_3)$	$\log(K_4)$	$\log(K_1K_2)$
CaM[b]	5.23 (0.14)	6.42 (0.20)	4.33 (0.31)	5.33 (0.20)	11.65 (0.15)
Acam	7.25 (0.40)	7.60 (0.35)	4.10 (0.45)	—	14.85 (0.35)
(+1 mM Mg^{2+})	6.73 (0.21)	6.81 (0.34)	<3.75	—	13.54 (0.24)
(+6 mM Mg^{2+})	5.94 (0.26)	6.34 (0.19)	<3.75	—	12.28 (0.21)

[a]The constants were determined in 10 mM Tris, 100 mM KCl (pH 8) at 20 °C. The values are the mean (±SD) from at least three determinations.
[b]Values from Martin et al. (1996).

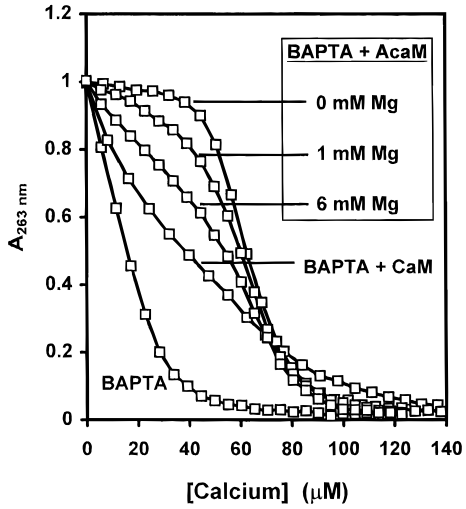

Fig. 3. Calcium binding to Acam and CaM. Typical experimental data for calcium titrations of 28.5 μM 5,5′-Br_2BAPTA alone and in the presence of 25 μM CaM or Acam. The titration with Acam was also performed in the presence of 1 and 6 mM $MgCl_2$. Titrations were performed at 20 °C in 10 mM Tris, 100 mM KCl, pH 8.0 (plus 1 mM DTT for Acam). The error on individual points is smaller than the size of the symbols. The total absorbance change has been normalized to facilitate comparison of the curves.

analyses thus indicate that Acam binds two calcium ions with very high affinity compared with CaM (the average affinity for the first two calcium ions, $(K_1K_2)^{1/2}$, is ~40-fold higher than for CaM) but that binding at a third (and possibly fourth) site is significantly weaker than with CaM. The binding of the first two calcium ions to Acam is clearly cooperative (because $K_2 > K_1$, see Linse et al., 1991) and the two high-affinity sites resemble a conventional pair of EF-hands, probably sites 3 and 4.

Calcium titrations of apo-Acam in the presence of either 1 or 6 mM $MgCl_2$ (cf., Ohki et al., 1997) show that magnesium causes a substantial reduction in K_1 and K_2 (K_3 is also reduced). These results are consistent with direct competition between magnesium and calcium for the available binding sites, as with CaM (Tsai et al., 1987; Ohki et al., 1997). The reduction in the average calcium affinity for the first two sites (~4.5- and 20-fold for 1 and 6 mM Mg^{2+}, respectively) suggests magnesium affinities in the range of $2–4 \times 10^3$ M^{-1}.

EGTA-induced dissociation of calcium was examined using stopped flow. The dissociation from holo-CaM was monitored using Tyr138, in EF-hand 4 in the C-terminus. The value of k_{obs} (3.8 ± 0.5 s^{-1}) is typical for dissociation of calcium from the C-terminal domain of CaM. k_{obs} for dissociation from the N-terminal domain is >500 s^{-1} at $T = 10$ °C (Martin et al., 1992; Brown et al., 1997). Dissociation from individual EF hands is not observed. Dissociation from holo-Acam was monitored using Trp142, in the F-helix of EF hand 4. k_{obs} was found to be 0.22 ± 0.06 s^{-1}, i.e., ~17-fold slower than for holo-CaM. These results suggest that EF-hand 4 is a high-affinity site in Acam and that the two high-affinity sites in Acam are EF-hands 3 and 4.

Near- and far-UV CD

Near-UV CD spectra of Acam are compared with those of CaM in Figure 4A. In CaM, the near UV-CD signal derives from Tyr138,

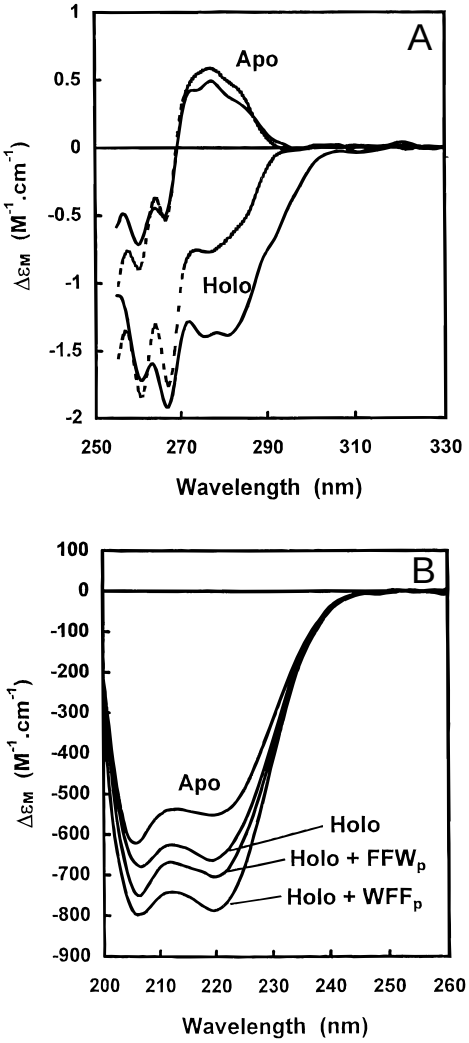

Fig. 4. A: Near-UV CD spectra of apo- and holo-forms of Acam and CaM. Spectra were recorded in 25 mM Tris, 100 mM KCl, pH 8.0 (plus 2.5 mM DTT for Acam) in 1 mM EGTA (apo) or 1 mM $CaCl_2$ (holo). The Acam spectra are shown as solid lines and the CaM spectra as dotted lines. **B:** Spectroscopic properties of Acam·peptide complexes. Far-UV CD spectra of apo- and holo-Acam, and of 1:1.1 mixtures of Acam (8 μM) with the peptides, WFF_p and FFW_p. Note: The FFW_p complex is not completely formed under the conditions of the experiment.

whereas in Acam Trp142 also contributes. The finding that the apo-forms have very similar spectra suggests that Tyr138 is in a very similar environment in the two proteins and that Trp142 in apo-Acam makes little contribution to the spectrum. The addition of calcium to apo-CaM results in major changes in the near-UV CD spectrum (cf., Maune et al., 1992a); thus, there is a significant calcium-induced change in the environment of Tyr138. Acam shows a similar overall change, but the difference between the two spectra shows that Trp142 makes a strong negative contribution to the holo-Acam signal, indicating strong calcium-dependent immobilization of this residue.

Far-UV CD spectra (Fig. 4B) show that apo-Acam has a high α-helical content. The increase in intensity in the presence of calcium indicates an increase in α-helical content upon calcium binding. The value of $\Delta\epsilon_{220\ nm}$ increases from −549 (apo) to

-664 M^{-1} cm^{-1} (holo-Acam); the values for CaM are -646 (apo) and -808 M^{-1} cm^{-1} (holo-CaM) (Maune et al., 1992a). Such comparisons are necessarily made under identical conditions of ionic strength, pH, and temperature, factors that influence the far-UV CD intensity (Martin & Bayley, 1986; Hennessey et al., 1987; Török et al., 1992; Browne et al., 1997). CaM has a slightly greater average α-helical content than Acam in both the apo- and holo-forms, and the maximal increase in α-helical content on binding calcium is ~40% greater for CaM. Both far- and near-UV spectra of Acam in the presence of excess Mg^{2+} (>2 mM) are indistinguishable from those of holo-Acam, showing that these metal ions induce similar changes in secondary and tertiary structure. This is a significant difference compared to CaM, which binds Mg^{2+} but without significant conformational change (Ohki et al., 1997)

Calcium and magnesium titrations

Three parameters were monitored during titration of Acam with calcium: (a) far-UV CD at 220 nm, (b) near-UV CD at 278 nm, and (c) integrated Trp fluorescence (290–450 nm), which decreases with calcium binding. Figure 5A shows that the near-UV CD and fluorescence signals, reflecting changes monitored by Tyr138 and Trp142 in the C-domain, vary linearly with $[Ca^{2+}]$ and saturate at $[Ca^{2+}]/[Acam] = 2$. The far-UV CD signal also varies linearly up 75% amplitude when $[Ca^{2+}]/[Acam] = 2$, but small further changes (25%) are seen as the ratio increases. These results are consistent with there being a major conformational change induced by calcium binding at two high-affinity sites in the C-terminal half of Acam. Titrating with magnesium induces similar overall changes in these optical properties (see Fig. 5B). The curves are consistent with the 5,5′-Br_2BAPTA titrations in showing magnesium binding to Acam with affinities in the range of 3–5 $\times$ 10^3 M^{-1}.

Thermal stability

The stability of Acam has been compared with that of CaM by monitoring thermally induced unfolding using CD (Fig. 6). Far-UV CD, which monitors secondary structure in both the N- and C-terminal lobes, reveals significant differences in the thermal stability of these proteins. Holo-CaM shows a monotonic change in signal up to 80 °C; calorimetry (Tsalkova & Privalov, 1985) showed the absence of a structural transition in this region, and studies on isolated holo-domains indicate they are stable up to 80 °C. By contrast, holo-Acam shows a well-defined transition with a midpoint, T_m of ~45 °C. Assuming that calcium binding to the Acam N-domain is weak, this transition is assigned to unfolding of the N-domain.

Apo-CaM shows a broad transition in far-UV CD between 25 and 70 °C, which corresponds in amplitude to complete unfolding of the protein. The slight inflection point suggests that the two domains have slightly different stabilities, but the transitions are not resolved. In the interpretation of Tsalkova and Privalov (1985), this broad transition of apo-CaM corresponds to overlapping transitions at 36 and 54 °C, representing the C- and N-terminal lobes, respectively. By contrast apo-Acam shows a biphasic curve, with two well-resolved transitions (Fig. 6A). In this case, the midpoint for the first transition is at ~25 °C and the second at ~55 °C. Analysis of the near-UV CD signals during heating resolved the relationship of these transitions to the unfolding of the two domains of the protein (see below).

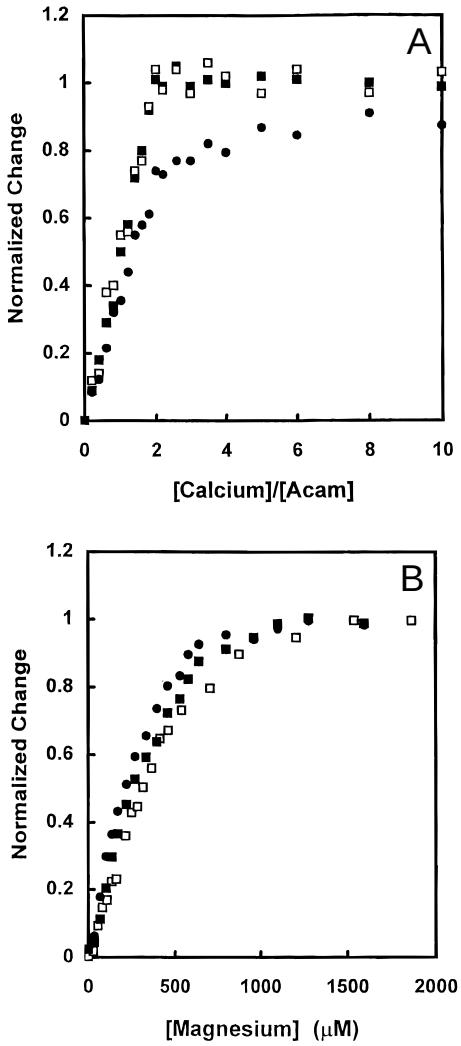

Fig. 5. Changes in spectroscopic parameters as a function of [calcium] and [magnesium]. **A:** Changes as a function of the [calcium]/[Acam] ratio monitored using near-UV CD ($\Delta\epsilon_{279\ nm}$, [Acam] = 150 μM, open squares), fluorescence emission (integrated fluorescence 300–490 nm, [Acam] = 20 μM, closed squares) and far-UV CD (220 nm, [Acam] = 20 μM, closed circles). The final values for the totally calcium-saturated form were taken to be the signals observed in 10 mM $CaCl_2$. **B:** Changes as a function of [magnesium] monitored using near-UV CD ($\Delta\epsilon_{279\ nm}$, [Acam] = 75 μM, open squares), fluorescence emission (integrated fluorescence 300–490 nm, [Acam] = 20 μM, closed squares) and far-UV CD (220 nm, [Acam] = 20 μM, closed circles). The final values for the totally calcium-saturated form were taken to be the signals observed in 10 mM $CaCl_2$.

The near-UV CD signals monitor the conformational properties of Tyr138 (CaM) and Tyr138 + Trp142 (Acam). Given that these residues are in the C-terminal regions of the proteins, they provide direct information on the stability of these regions. For holo-CaM, the signal decreases monotonically (by approximately 40%) over the range 10 to 80 °C, but no major unfolding is observed, showing that the C-terminal lobe of holo-CaM only unfolds at $T > 85$ °C (Fig. 6B). In apo-CaM, the C-terminal half is much less stable, and the signal is lost in a single broad transition with an apparent midpoint of ~42 °C (Fig. 6B). The behavior of Acam is similar to that of CaM. There is no evidence of a structural transition with holo-Acam, and apo-Acam shows a single broad transition with

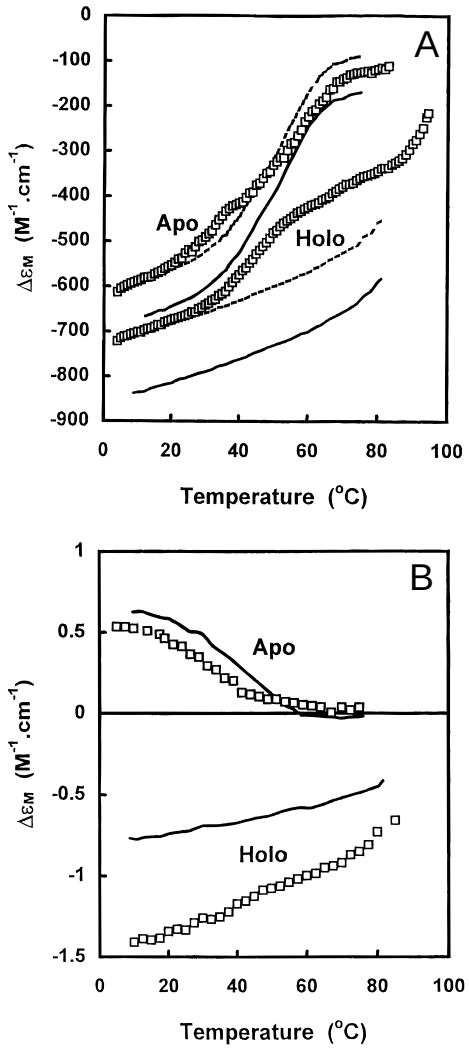

Fig. 6. Thermal unfolding of Acam and CaM. **A:** Changes in far-UV CD signals at 220 nm for Acam (open squares) and CaM (solid lines). Dotted lines are the data for CaM offset by +80 (apo) and +130 (holo). Spectra were recorded at a concentration of 7.5 μM in 25 mM Tris, 100 mM KCl, pH 8.0 (plus 2.5 mM DTT for Acam) with 1 mM EGTA or 1 mM $CaCl_2$. **B:** Changes in near-UV CD signals at 278 nm for Acam (open squares) and CaM (lines). Spectra were recorded at a concentration of 150 μM in 25 mM Tris, 100 mM KCl, pH 8.0 (plus 2.5 mM DTT for Acam) with 1 mM EGTA (apo) or 1 mM $CaCl_2$ (holo-Acam).

$T_m \sim 30$ °C. Thus, the C-domain of Acam strongly resembles that of CaM in its thermal stability and in the degree of stabilization conferred by binding calcium. The finding from near-UV CD that the Acam C-terminal domain unfolds with a transition at ~30 °C indicates that the transition for apo-Acam at ~25 °C seen in the far-UV CD also represents C-domain unfolding, and, thus, that the far-UV CD transition at ~55 °C must be attributed to the N-domain. As described above, the N-domain unfolds in the presence of 1 mM $CaCl_2$ at a significantly lower temperature (~45 °C). Thus, taken together, these findings suggest that, in the absence of calcium, the prior unfolding of the C-domain can provide some stabilization of the N-domain against unfolding, implying that an interaction of the unfolded (apo) C-domain with the folded (apo) N-domain can occur in Acam. The most significant results are that Acam shows a two-domain behavior and that the C-domain is markedly stabilized by the high affinity binding of calcium ions.

The affinity of Acam for typical target peptides

We have measured the affinity of Acam for four peptides related to the CaM target sequence of native sk-MLCK and a high-affinity synthetic peptide (CBP1), as used in previous studies with CaM (Findlay et al., 1995b; Martin et al., 1996; Bayley et al., 1996; Brown et al., 1997). For the spectroscopically silent peptides (CBP1 and FFF_p), the fluorescence increase of Trp142 in holo-ACam was measured upon adding the peptide to a solution of the protein. Otherwise, the intensity at 325 or 330 nm was measured on adding holo-Acam to a solution of the peptide, based on the blue shift and intensification of the peptide Trp on complex formation.

All of the peptides studied bind to holo-Acam much more weakly (between 10^3- and 10^5-fold) than to CaM (Table 2). For the two WFF peptides, the blue shift and intensification observed upon complex formation are very similar to those for CaM (20–22 nm blue shift, approximately threefold enhancement at 335 nm). In the case of FFW_p, the blue shift upon complex formation with Acam (~9 nm) is much smaller than with CaM (~21 nm); the intensification is also much lower in the complex with holo-Acam.

Peptide affinities were also measured for Mg-Acam and apo-Acam. The optical properties of the complexes of the peptides with Mg-Acam are similar to those described above for complexes with holo-Acam, for both the spectroscopically silent and the Trp-containing peptides. The affinities of the peptides for Mg-Acam are also very similar to those for holo-Acam. The affinities of apo-Acam for the peptides are not significantly lower than those of

Table 2. *Dissociation constants for the binding of target peptides to CaM and Acam*[a]

	holo-CaM K_d (pM)[b]	holo-Acam K_d (μM)	Mg-Acam K_d (μM)	apo-Acam K_d (μM)	K_d ratio[c]
CBP1	5	0.85 (0.15)	1.25 (0.25)	1.50 (0.30)	1.7×10^5
FFF_p	40	0.45 (0.10)	0.35 (0.10)	1.15 (0.25)	1.125×10^4
FFW_p	130	1.85 (0.35)	2.40 (0.40)	8.50 (3.50)	1.40×10^4
WFF_p	1.5	0.06 (0.01)	0.08 (0.02)	1.05 (0.25)	4.0×10^4
WFF_u	145	0.21 (0.04)	0.25 (0.05)	1.70 (0.55)	1.45×10^3

[a]The constants were determined in 25 mM Tris, 100 mM KCl (pH 8) at 20 °C. The values quoted are the mean (±SD) from at least three determinations.

[b]Methods used to determine these constants will be described elsewhere (S.R. Martin & P.M. Bayley, in prep.).

[c]The K_d ratio is K_d(holo-Acam)/K_d(holo-CaM).

holo-Acam, except in the case of WFF_p. The fluorescence properties of the complexes with apo-Acam are also similar to those described for holo-Acam, except that the complexes with the WFF peptides were characterized by small blue shifts (6–8 nm) and small intensifications.

The spectroscopic results show that holo-Acam binds to the WFF peptides with the same orientation as does CaM, i.e., with the peptide Trp interacting with the C-domain. The substantial reduction in affinity of Acam for the MLCK peptides is surprising in view of the close similarity of the C-domains in CaM and Acam. The value of K_d for WFF_u with holo-Acam (0.21 μM) may be compared with values of 0.73 μM for the interaction of $WF10_u$ (the first 10 residues of WFF_u) with holo-CaM and 0.076 μM for the interaction of WFF_u with Tr2C, the C-domain of CaM (Bayley et al., 1996). These results suggest the possibility that the N-terminal portion of Acam, even in the presence of calcium, shows little or no affinity for the C-terminal portion of the WFF_u peptide. Clearly, there is a significant difference in target specificity and action of Acam compared to CaM. This deduction is consistent with the exclusive location of Acam in the testis, fulfilling a role independent of CaM, although the latter is also present and active in this tissue.

Conformational properties of Acam:peptide complexes

We have previously shown that the sk-MLCK peptides generate characteristic near-UV CD difference spectra upon binding to holo-CaM (Findlay et al., 1995a; Bayley et al., 1996; Barth et al., 1997). In particular, holo-CaM-WFF_u (in which Trp4 interacts predominantly with the C-terminal lobe of CaM) has an intense positive near-UV CD difference spectrum, whereas holo-CaM-FFW_u (in which Trp-17 interacts with the N-terminal lobe of CaM; see Findlay et al., 1995a) has an intense negative difference spectrum.

In complexes of holo-Acam with the WFF peptides, the near-UV CD difference spectrum is closely similar in intensity to that for holo-CaM, suggesting a similar environment for the peptide Trp4 residue in the two complexes, with the contribution to the CD of the Trp142 of Acam being unaffected by peptide binding. Consistent with this, the fluorescence of Trp4 is blue shifted and intensified upon binding to holo-Acam in much the same way as it is with holo-CaM. The complex of WFF_p with Mg-Acam has a difference spectrum that is indistinguishable from that produced with holo-Acam. In the case of apo-Acam, complex formation with the WFF peptides did not generate a difference spectrum, consistent with the fluorescence results.

In contrast, the complexes of FFW_p with holo-Acam, Mg-Acam, and apo-Acam show virtually no Trp CD difference spectrum, so that the peptide Trp environment must be very different in the complexes with Acam compared to CaM. Finally, we note that the formation of the complex of holo-Acam and FFF_p has little effect on the near-UV CD spectrum of the Acam, confirming that the Trp142 contribution to the Acam CD spectrum is unchanged by peptide binding.

The free peptides have little regular secondary structure; their far-UV CD spectra show intense negative bands below 198 nm, and only low intensity at longer wavelengths. The increase in far-UV CD intensity on peptide binding is consistent with the peptide adopting a predominantly α-helical structure in the complex. Peptide binding generally has little effect on CaM helicity (Crivici & Ikura, 1995). The number of additional peptide residues in a helical conformation in the complex (n_H), calculated from the change in CD at 222 nm (Findlay et al., 1995b; Bayley et al., 1996), are compared for CaM and Acam in Table 3. Assuming these are attributable to peptide, in the complexes with holo-Acam, the WFF_p peptide becomes significantly helical, and the FFW_p and FFF_p peptides less so.

Molecular modeling of the androcam sequence

Given the degree of homology between Acam and CaM (Fig. 1), modeling studies were initiated to assess if there are key substitutions in Acam that might prevent the adoption of a conformation closely similar to that of CaM. Figure 1 shows that there are no extensive continuous stretches of residues that are significantly different between the proteins. In the first EF hand (CaM numbers 20–31), residues at positions 5, 7, and 9 in the calcium-binding loop are nonhomologous, but these are the less strongly conserved positions of the loop (Falke et al., 1994). In the second EF hand (56–67), there are significant changes of key conserved residues in positions 1, 3, and 4 of the loop (D56E, D58N, G59N). There are also changes at loop positions 2, 7, 9, and 11, and a further three changes at residues 69–71, part of the short helix (residues 66–73). In sites 3 and 4, there are changes at nonconserved positions (N97D, A102P, I130F, and Q135M).

The Acam sequence was threaded onto the consensus structures of CaM using comparative homology modeling with the Swiss-Model software (Guex & Peitsch, 1997), incorporating the GROMOS force-field (van Gunsteren et al., 1996) for a local refinement using energy minimization of the initial derived structure. Two separate threading processes were performed for the Acam sequence—one based on holo-CaM template structures 1cll, 1osa, and 4cln (X-ray diffraction), and one on apo-CaM structures, 1cfc and 1dmo (NMR). Resulting structures for holo- and apo-Acam were compared against the template structures and examined for stereochemical quality using WHATIF (Vriend, 1990). For both holo- and apo-Acam, acceptable structures were obtained, lacking any stereochemical violations, as indicated by Z-values comparable to the template structures. In this threading procedure, the polypeptide backbone conformation necessarily remains similar to

Table 3. *Far-UV CD extinction coefficients (222 nm) for complexes of CaM and Acam with model target peptides*

	holo-Acam		holo-Cam	
Peptide	$\Delta\Delta\epsilon_M$[a] (M^{-1} cm^{-1})	n_H[b]	$\Delta\Delta\epsilon_M$ (M^{-1} cm^{-1})	n_H
WFF_p	−121 (10)	11.3 (1)	−138 (10)	12.9 (1)
FFF_p	−65 (10)	5.9 (1)	−134 (10)	12.6 (1)
FFW_p	−73 (10)	6.7 (1)	−139 (10)	13.1 (1)

[a] CD extinction coefficients ($\Delta\epsilon_M$) were measured in 25 mM Tris, 100 mM KCl (pH 8) at 20 °C. $\Delta\Delta\epsilon_M$ was calculated using $\Delta\Delta\epsilon_M = \Delta\epsilon_M$(Complex) − $\Delta\epsilon_M$(protein), with $\Delta\epsilon_M$(holo-CaM) = −808 M^{-1} cm^{-1} and $\Delta\epsilon_M$(holo-Acam) = −664 M^{-1} cm^{-1}. The values for Acam with FFW_p and FFF_p have been corrected for the presence of uncomplexed peptide using the dissociation constants given in Table 2. Estimated errors are given in parentheses.

[b] The number of additional peptide bonds adopting a helical conformation upon complex formation was calculated as described in Bayley et al. (1996).

that of the template structures. The RMS difference between apo-Acam and 1cfc was 0.2 for the backbone of the total sequence and 0.2 for either the N- or C-domain. The holo-Acam model structure shows an RMS difference of 0.5 for the backbone sequence compared to 1cll and 0.5 for the N-domain and 0.4 for the C-domain comparisons. Thus, the Acam sequence can be be accommodated with relatively few conformational adjustments compared to the structure of CaM, and it can be concluded that, at the level of this approach, there are no individual residues exerting a dominant structural perturbation that would account for the observed difference in conformational properties of Acam. Preliminary results from an extended molecular dynamics simulation using Biosym software, and explicitly considering the interactions of the Ca ions, indicates that the changes in ligands in site 1 (D24T) and site 2 (D56E) make significant contributions to differences in affinity and loop conformation in Acam.

The dynamic properties of the two derived structures were investigated using essential dynamics simulation procedures (de Groot et al., 1997). This procedure efficiently mimics effects of a long-term molecular dynamic simulation by statistical generation of a family of conformations on the basis of a list of distance bounds, which is generated from a chosen starting structure. A comparison of apo-Acam and apo-CaM revealed a significantly higher mobility of the sequence stretch 28–57, which is the region including helix B and helix C. Additionally, helix G (residues 117–128) showed higher mobility. This higher flexibility of secondary structure elements is indicative of the potential for a loss of secondary structure content, consistent with the experimental observations, but the methods do not at this stage treat the process of major changes of backbone conformation.

Discussion

Correlation of the EF hands of Acam with the three calcium-binding sites detected experimentally

Although Acam contains four EF-hand motifs with calcium-binding loops analogous to those of CaM (EF1–EF4 in Fig. 1), only three of these are functional in calcium binding. Two of these sites show pronounced cooperativity and an even greater average calcium affinity than the two high-affinity sites in CaM. Spectroscopic data, based on the properties of Tyr138 and Trp142, clearly favor the high-affinity sites as being the two C-domain EF hands of Acam (equivalent to the two high-affinity sites EF3 and EF4 of CaM). Further, these two sites show strong sequence conservation when compared to CaM.

Binding data does not permit unequivocal identification of the nonfunctional site within the N-domain of Acam, but sequence comparisons to CaM suggest that site EF2 is likely to be impaired in calcium affinity, and more extensive conformational effects in this region are implied by the MD calculations. In this case, binding at EF1 could also be weakened owing to effects on the cooperativity between EF1 and EF2. Biekofsky et al. (1998) have shown that site occupancy of EF hands can be monitored with HSQC-NMR calcium titrations, and this approach can be utilized to assign calcium binding to Acam unambiguously.

Calcium-induced conformational changes in Acam

Thermal unfolding studies demonstrate that Acam, like CaM, has a two-domain structure and that calcium greatly stabilizes the C-terminal domain. The conformational effect of binding calcium to Acam is an increase in α-helical content, resembling but smaller than that for CaM. However, like CaM this effect is mainly in the C-domain. Both apo- and holo-Acam are lower in α-helical content than apo- and holo-CaM, respectively, even when the comparison is made at low temperatures ($\sim$5 °C) to allow for the intrinsically lower stability of Acam. In addition, a tryptic cleavage site present in the apo-forms of CaM and Acam (Arg37 and Arg36, respectively) is retained in holo-Acam. Thus, significant structural differences probably exist between the calcium-bound forms of Acam and CaM and the sequence changes underlying the loss of calcium binding in the N-domain of Acam may be the major determinants of these conformational effects. The sequences of Acam least homologous to CaM are the calcium-binding loop and F-helix of EF2, and it is possible that these dictate a different local conformation in this region of the protein, and perhaps also produce a different disposition of the N- and C-domains, in addition to loss of calcium binding at EF2. This is also consistent with the altered interaction of Acam with sk-MLCK peptides. The fluorescence data strongly suggest that the C-domain of Acam interacts with the N-terminal sequence of the peptides in a comparable orientation to the M13-CaM complex (Ikura et al., 1992; cf., Meador et al., 1992, 1993). However, there is little evidence for an interaction of the N-domain of Acam with the C-terminal region of the peptides. Because the natural targets of Acam have not yet been identified, it is premature to put too much emphasis on these extrapolations, but it appears that significant differences will underlie the altered calcium-binding properties of Acam and also produce altered target specificity.

The molecular modeling is of interest from the point of view of the large number of CaM-like and other EF-hand calcium-binding proteins, which show specificities of biological function that cannot be substituted by CaM itself. A priori, one might expect examples to be found of proteins where changes in conformation occur due to single substitutions. These have potentially far-reaching consequences, as typified by the large effect on domain stability of the substitution by Gly of the hydrophobic residues Ile or Val at position 8 of any the calcium-binding loops of CaM (Browne et al., 1997). By contrast, Acam appears to be an example of an alternative situation, in which the change of properties compared to CaM is due to the cumulative effect of several substitutions, none of which appears to be obviously critical, although the changes in liganding in sites 1 and 2 do appear significant. This type of cumulative variation has an important difference, because the number of residues involved is larger, and the effect is more likely to be exhibited as a change in a surface property, which could confer target specificity. Also, this cumulative effect would not readily be compensated or reversed by a simple process such as the binding of a ligand, for example, a target sequence or calcium ion (Browne et al., 1997), and hence, would confer greater specificity, owing to the stronger differentiation of the CaM-like protein from the parent molecule.

It is interesting that the region of Acam showing the greatest potential difference from CaM appears to be located at the surface of the molecule. This would enable the maximum opportunity for specific secondary interactions involved in target recognition. It is now clear that, in addition to the specific primary site of interaction of CaM with targets, other areas of the protein may confer additional specificity via interactions of its surface residues (Persechini et al., 1996; Krueger et al., 1998), and it is reasonable to suggest that this might be involved in the mechanism of the differential and specific action of Acam.

The significance of magnesium binding to Acam

The relative affinity for calcium vs. magnesium for tight binding to the C-domain of Acam is similar to that for CaM. To date, no significant difference has been observed in the equilibrium conformational response of Acam to saturating concentrations of calcium as opposed to magnesium. The CD and fluorescence data suggest that either calcium or magnesium cause a similar change in secondary and tertiary structure of the C-domain of Acam. This behavior contrasts sharply with that of CaM, where magnesium binds competitively with calcium but without producing conformational effects (Ohki et al., 1997). Although cation preference in either domain may clearly be modified by interaction with target proteins, this difference in conformational response of Acam presents the following possibility: at physiological magnesium levels (~5 mM) and resting calcium levels (below 0.1 μM) the C-domain of Acam could be at least partially occupied by magnesium with a conformation close to that of the holo-form. This situation would be somewhat analogous to that for troponin C, the C-domain sites of which are thought to be occupied by magnesium in resting muscle. Like troponin C, Acam could be bound but with a nonactivating role in this calcium-independent state. A kinetic preference for calcium over magnesium as calcium levels are rapidly increased might then lead to transient calcium occupation of the C-domain sites, a relatively subtle conformational change (possibly involving the N-domain), and activation of appropriate targets. As for CaM, physiological levels of magnesium are predicted to moderate the high calcium affinity of Acam. Assuming that in the testis CaM and Acam are affected similarly by magnesium, as in vitro, the higher calcium affinity of Acam would prevail.

Is Acam a calcium sensor in vivo?

If differences in calcium affinity between Acam and CaM persist in the testis, one prediction from the studies presented here is that calcium occupancy of the EF hands on Acam will take place over ranges of calcium concentrations differing significantly from the response range of CaM. Thus, in vitro in the absence of magnesium, the average calcium dissociation constant for the strong binding sites of Acam is ~0.04 μM, and that of the weak site 100 μM, whereas the corresponding values for the strong and weak sites of CaM are 0.15 and 15 μM, respectively (Martin et al., 1996). If Acam were to act as a calcium sensor, the interesting implication is that it could extend the calcium response range in the testis into both lower and/or higher calcium levels than those detectable by CaM. Whether Acam would act as a sensor for calcium concentrations both below and above the CaM response range would depend upon the degree to which interaction of Acam with target proteins affects the apparent affinity for calcium binding in the N- and/or C-domains.

Although, to our knowledge there has been no quantitation of calcium (or magnesium) levels in developing or mature sperm, studies of both resting and response-related calcium levels in other systems (see Bootman & Berridge, 1995) would tend to argue against the hypothesis that any of the calcium-binding sites on Acam has a calcium-sensing function. Thus, the normal response-related increases in intracellular calcium would be insufficient to produce occupancy of the weak binding site on Acam, and given that resting calcium levels can be as high as 0.1 μM, in the absence of a competing ion the high-affinity sites of Acam could well be constitutively occupied with calcium. An extreme alternative view, therefore, would be that the weak site on Acam is not functional in vivo, and that the high-affinity sites have a constitutive role, comparable to the homologous sites on troponin C, and act to produce a permanent conformation, perhaps required for interaction with some other protein moiety. However, in the presence of a target sequence, which interacts in a calcium-dependent manner with both domains of Acam (or even interacts solely with the N-domain), the apparent calcium-affinity of the N-domain could be enhanced by several orders of magnitude (cf., Olwin & Storm, 1985; Yazawa et al., 1992; Bayley et al., 1996; Peersen et al., 1997).

Despite these uncertainties, studies of sea urchin sperm motility provided evidence that supports the idea of a calcium sensing-function for Acam, potentially for both its high- and low-affinity sites (Brokaw, 1991). Asymmetry in the sperm flagellar bending waves appears to be regulated by at least two calcium sensors, one of which operates at calcium concentrations below the response range of CaM, and the other at the high end of CaM's range. Attempts to demonstrate that either of these sensors was CaM were unsuccessful, leaving the possibility that one or both responses reflect the action of a sensor similar to Acam.

Materials and methods

Proteins and peptides

The scheme used to generate the IPTG-inducible bacterial expression construct for Acam (pET15b-Acam) is described in the electronic supplementary material. The pET15b-Acam construct was transformed into *Escherichia coli* strain BL21(DE3pLys). Optimal expression of Acam was obtained by induction with 60 mM IPTG for 2–4 h. Bacterial lysates were prepared as described by Maune et al. (1992b), except that 1 mM DTT was included in the lysis buffer. Acam was purified from the lysates by phenyl-sepharose affinity chromatography using high salt (500 mM NaCl) conditions as described previously (Maune et al., 1992b), with the inclusion of 1 mM DTT in all solutions. Purity of column elution fractions was assessed by SDS-PAGE electrophoresis and spectral properties. One or two repeat rounds of phenyl-sepharose chromatography were sometimes required for complete purification. *Drosophila* CaM was expressed in *E. coli* and purified as described elsewhere (Maune et al., 1992b; Browne et al., 1997). CaM and Acam were made calcium-free by incubating with 5–25 mM EGTA and then desalting by passage though two Pharmacia PD10 (G25) columns equilibrated with Chelex-treated buffer (25 mM Tris, 100 mM KCl, pH 8.0, plus 2.5 mM DTT for Acam).

Peptides WFF (KRR**W**KK-N**F**IAVSAANR**F**K), FFW (KRR **F**KKN**F**IAVSAANR**W**K), FFF (KRR**F**KKN**F**IAVSAANR**F**K), and CBP1 (Ac-LKLKKLLKLLKKLLKLG-NH_2) were prepared as described (Findlay et al., 1995b). WFF is the first 18 residues of M13, the CaM target sequence of sk-MLCK; FFW and FFF are variants of this sequence. Unprotected and protected peptides (with N-terminal acetylation and C-terminal amidation) are shown with subscripts u and p, respectively. Concentrations were determined spectrophotometrically using $\epsilon_{280} = 5{,}690\ M^{-1}\ cm^{-1}$ for WFF and FFW (Gill & von Hippel, 1989), $\epsilon_{259} = 585\ M^{-1}\ cm^{-1}$ for FFF (Gill & von Hippel, 1989), $\epsilon_{279} = 1{,}578\ M^{-1}\ cm^{-1}$ for holo-CaM (Maune et al., 1992b), and $\epsilon_{280.5} = 7{,}173\ M^{-1}\ cm^{-1}$ for holo-Acam or $\epsilon_{279.5} = 7{,}073\ M^{-1}\ cm^{-1}$ for apo-Acam. The extinction coefficients for Acam were determined as for CaM (Maune et al., 1992b; cf., Edelhoch, 1967), using the assumption that the extinction coefficient of the fully denatured protein is the same as that for a

mixture of aromatic amino acid esters in the same molar ratio as in the protein. Acam contains 1 Trp, 1 Tyr, and 11 Phe residues. A 1:1:11 mol ratio mixture of the methyl esters of Trp, Tyr, and Phe was therefore used.

Tryptic digestion studies

Decalcified aliquots (10 μg) of Acam in 5 mM Tris, pH 8.0, 0.1 mM EDTA, and 1 mM DTT were subjected to digestion with TPCK-treated trypsin (Sigma, St. Louis, Missouri) as described by Walsh et al. (1977) in the presence of 1 mM EDTA or various concentrations of $CaCl_2$ (0.1–20 mM). Trypsin:Acam ratios of 1:50–5,000 were investigated. Reactions were stopped by adding 4×-SDS sample buffer and boiling briefly. Digests were analyzed by standard SDS-gel electrophoresis on 12 or 15% gels. For N-terminal sequencing, peptides from scaled-up electrophoretic runs were electroblotted to PVDF membrane (Bio-Rad, Hercules, California) in 10 mM CAPS, pH 11.0, containing 10% methanol, 0.1 M thioglycolate, and 1 mM $CaCl_2$. After transfer, peptides were fixed onto the membrane with 0.2% glutaraldehyde and stained with 0.1% Amido Black. The desired bands were cut out and eluted with 50% ethanol. N-terminal sequencing by the automated Edman degradation was performed on Applied Biosystems Sequencing Systems 473A or 477A in the Protein Chemistry Core Laboratory of Baylor College of Medicine.

The N-terminal sequence of peptide C1 (Fig. 2) was TLGQNPTEAE, unequivocally identifying the first cleavage in the presence of calcium as occurring after R36 of Acam. The N-terminal sequences of the first peptides generated in the presence of EDTA (E1 and E2, Fig. 2) were (-ELTEEQIAE) and (FVMINLGE-VT), respectively, indicating that the initial cleavage in the absence of calcium is after R105. Peptide E3, which is derived from E1 on longer digestion, has the same N-terminal sequence as E1, indicating that it is generated by secondary cleavage in the C-terminal region of E1.

Calcium binding studies

Stoichiometric calcium association constants for Acam were determined from calcium titrations of apo-Acam performed in the presence of the chromophoric chelators, 5,5′-Br_2BAPTA and Quin-2, using published methods (Linse et al., 1988, 1991; Martin et al., 1996). Measurements were made at 20 °C in 10 mM Tris, 100 mM KCl, 1.0 mM DTT, pH 8.0; under these conditions the calcium binding constants of 5,5′-Br_2BAPTA and Quin 2 are 5.7×10^5 M^{-1} and 1.1×10^7 M^{-1} (Martin et al., 1996). Titrations were also performed using 5,5′-Br_2BAPTA in the presence of 1 and 6 mM Mg^{2+}; this does not interfere with the assay, because the association constant of the chelator with Mg^{2+} is <5 M^{-1} under these conditions (S.R. Martin, unpubl. obs.). Three separate titrations were performed on each protein sample, and the values for the individual binding constants were obtained from nonlinear least-squares fits directly to the experimentally observed titration curves. Stopped-flow kinetic measurements were performed with a Hi-Tech SF61-MX stopped-flow spectrophotometer (λ_{ex} = 280 nm for CaM Tyr138 fluorescence and 290 nm for Acam Trp142 fluorescence with 305 or 320 nm cuton emission filters). Measurements were made in 25 mM Tris, 100 mM KCl, 2.5 mM DTT, 1 mM $CaCl_2$, and pH 8.0 buffer at 10°C.

CD and fluorescence measurements

CD spectra of Acam and Acam·peptide complexes were recorded on a Jasco J-600 spectropolarimeter at 20 °C in 25 mM Tris, 100 mM KCl, 2.5 mM DTT, and pH 8.0 (plus 1 mM $CaCl_2$ or 2–10 mM $MgCl_2$ when appropriate) as described elsewhere (Findlay et al., 1995b; Bayley et al., 1996). Spectra are presented as the CD absorption coefficient calculated using the molar concentration of peptide or protein ($= \Delta\epsilon_M$) rather than on a mean residue weight (mrw) basis. Values of $\Delta\epsilon_{mrw}$ may be calculated as $\Delta\epsilon_{mrw} = \Delta\epsilon_M/N$, where N is the number of peptide bonds (= 147 or 146 for CaM or Acam). For the sk-MLCK peptides, $N = 17$ for the unprotected form and 19 for the protected form. The number of peptide bonds in a helical conformation n_H was calculated from $\Delta\epsilon_M$ at 222 nm as described (Findlay et al., 1995a). CD changes as a function of temperature were studied in 10 mm cuvettes with direct temperature monitoring; measurements were made at protein concentrations of 7.5 μM (far-UV) and 150 μM (near-UV) in buffers with 1 mM (or 5 mM) $CaCl_2$ or 1 mM EGTA. Heating rates of ~1 °C/min were used over the range 5 to 90 °C. Thermal unfolding profiles reported were >95% reversible. Uncorrected Trp emission spectra of Acam and Acam·peptide complexes were recorded at 20 °C in 25 mM Tris, 100 mM KCl, 2.5 mM DTT, and pH 8.0 (plus 1 mM $CaCl_2$ or 1 mM EGTA) using a SPEX FluoroMax fluorimeter with λ_{ex} = 280 or 290 nm (bandwidth 1.7 nm) and emission from 310 to 450 nm (bandwidth 5 nm).

Determination of peptide affinities

Dissociation constants for WFF and FFW were determined by direct fluorometric titration of peptide with Acam in 25 mM Tris, 100 mM KCl, 2.5 mM DTT, 1 mM $CaCl_2$, and pH 8.0 (cf. Findlay et al., 1995b). Dissociation constants for FFF and CBP1 were determined by titration of Acam with peptide, monitoring the changes in the fluorescence of Trp142 in Acam. Data were analyzed using the method of Marquardt (Bevington, 1969). Three independent titrations were performed in each case and the average value is reported with its standard deviation.

Supplementary material in Electronic Appendix

The supplementary material describes the scheme used to generate the IPTG-inducible bacterial expression construct for Acam (pET15b-Acam).

Acknowledgments

These studies were supported by NIH Grant GM 49155 and Grant C-1119 of the Robert A. Welch Foundation of Texas to K.B. and a Nettie S. Autrey Fellowship to A.Q.L.

References

Andres AJ, Thummel CS. 1995. The *Drosophila* 63f early puff contains e63-1, an ecdysone-inducible gene that encodes a novel Ca^{2+}-binding protein. *Development 8*:2667–2679.

Barth A, Martin SR, Bayley PM. 1997. Specificity and symmetry in the interaction of calmodulin domains with the skeletal myosin light chain kinase target sequence. *J Biol Chem 273*:2174–2183.

Bayley PM, Findlay WA, Martin SR. 1996. Target recognition by calmodulin: Dissecting the kinetics and affinity of interaction using short peptide sequences. *Protein Sci 5*:1215–1228.

Bevington PR. 1969. *Data reduction and error analysis for the physical sciences.* New York: McGraw-Hill.

Biekofsky RR, Martin SR, Browne JP, Bayley PM, Feeney J. 1998. Ca^{2+} coordination to backbone carbonyl oxygen atoms in calmodulin and other EF-hand proteins: ^{15}N chemical shifts as probes for monitoring individual-site Ca^{2+} coordination. *Biochemistry 37*:7617–7629.

Bootman MD, Berridge MJ. 1995. The elemental principles of calcium signaling. *Cell 8*:675–678.

Brokaw CJ. 1991. Calcium sensors in sea-urchin sperm flagella. *Cell Motil Cytoskel 18*:123–130.

Brown SE, Martin SR, Bayley PM. 1997. Kinetic control of the dissociation pathway of calmodulin–peptide complexes. *J Biol Chem 272*:3389–3397.

Browne JP, Strom M, Martin SR, Bayley PM. 1997. The role of β-sheet interactions in domain stability, folding, and target recognition reactions of calmodulin. *Biochemistry 36*:9550–9561.

Cohen P, Klee CB. 1988. *Calmodulin*. Amsterdam: Elsevier Science Publishers B.V.

Crivici A, Ikura M. 1995. Molecular and structural basis of target recognition by calmodulin. *Annu Rev Biophys Biomol Struct 24*:85–116.

de Groot BL, van Aalten DMF, Scheek RM, Amadei A, Vriend G, Berendsen HJC. 1997. Prediction of protein conformational freedom from distance constraints. *Proteins Struct Funct Genet 29*:240–251.

Doyle KE, Kovalick GE, Lee E, Beckingham K. 1990. *Drosophila-melanogaster* contains a single calmodulin gene—Further structure and expression studies. *J Mol Biol 213*:599–605.

Edelhoch H. 1967. Spectroscopic determination of tryptophan and tyrosine in proteins. *Biochemistry 6*:1948–1954.

Falke JJ, Drake SK, Hazard AL, Peersen OB. 1994. Molecular tuning of ion binding to calcium signaling proteins. *Q Rev Biophys 27*:219–290.

Findlay WA, Gradwell MJ, Bayley PM. 1995a. Role of the N-terminal region of the skeletal muscle myosin light chain kinase target sequence in its interaction with calmodulin. *Protein Sci 4*:2375–2382.

Findlay WA, Martin SR, Beckingham K, Bayley PM. 1995b. Recovery of native structure by calcium binding site mutants of calmodulin upon binding of sk-MLCK target peptides. *Biochemistry 34*:2087–2094.

Fyrberg C, Parker H, Hutchinson B, Fyrberg E. 1994. *Drosophila-melanogaster* genes encoding 3 troponin-c isoforms and a calmodulin-related protein. *Biochem Genet 32*:119–135.

Gill SC, von Hippel PH. 1989. Calculation of protein extinction coefficients from amino acid sequence data. *Anal Biochem 182*:319–326.

Guex N, Peitsch MC. 1997. SWISS-MODEL and the Swiss-PdbViewer: An environment for comparative protein modelling. *Electrophoresis 18*:2714–2723.

Hennessey JP, Manavalan P, Johnson WC, Melencik DA, Anderson SR, Schimerlik MI, Shalitin Y. 1987. Conformational transitions of calmodulin as studied by vacuum-UV CD. *Biopolymers 26*:561–571.

Ikura M, Clore GM, Gronenborn AM, Zhu G, Klee CB, Bax A. 1992. Solution structure of a calmodulin–target peptide complex by multidimensional NMR. *Science 256*:632–638.

Kawasaki H, Kurosu Y, Kasai H, Isobe T, Okuyama T. 1986. Limited digestion of calmodulin with trypsin in the presence or absence of various metal ions. *J Biochem 99*:1409–1461.

Kretsinger RH. 1980. Structure and evolution of calcium-modulated proteins. *CRC Crit Rev Biochem 8*:119–174.

Krueger JK, Zhi G, Stull JT, Trewhella J. 1998. Neutron-scattering studies reveal further details of the Ca^{2+}/calmodulin-dependent activation mechanism of myosin light chain kinase. *Biochemistry 37*:13997–14006.

Linse S, Brodin P, Johansson C, Thulin E, Grundstrom T, Forsen S. 1988. The role of surface charges in ion binding. *Nature 335*:651–652.

Linse S, Helmersson A, Forsen S. 1991. Calcium binding to calmodulin and its globular domains. *J Biol Chem 266*:8050–8054.

Lu A, Beckingham K. 1997. Androcam: A male-specific calmodulin homolog in *D. melanogaster*. *38th Annual Drosophila research conference*. Abstract 128C.

Mackall J, Klee CB. 1991. Calcium-induced sensitization of the central helix of calmodulin to proteolysis. *Biochemistry 30*:7242–7247.

Martin SR, Bayley PM. 1986. The effect of Ca^{2+} and Cd^{2+} on the secondary and tertiary structure of calmodulin. *Biochem J 238*:485–490.

Martin SR, Bayley PM, Brown SE, Porumb T, Zhang M, Ikura M. 1996. Spectroscopic characterization of a high-affinity calmodulin-target peptide hybrid molecule. *Biochemistry 35*:3508–3517.

Martin SR, Maune JF, Beckingham K, Bayley PM. 1992. Stopped-flow studies of calcium dissociation from calcium-binding-site mutants of *Drosophila melanogaster* calmodulin. *Eur J Biochem 205*:1107–1114.

Maune JF, Beckingham K, Martin SR, Bayley PM. 1992a. Circular-dichroism studies on calcium-binding to 2 series of Ca^{2+} binding-site mutants of *Drosophila-melanogaster* calmodulin. *Biochemistry 31*:7779–7786.

Maune JF, Klee CB, Beckingham K. 1992b. Ca^{2+} binding and conformational change in two series of point mutations to the individual Ca^{2+}-binding sites of calmodulin. *J Biol Chem 267*:5286–5295.

Meador WE, Means AR, Quiocho FA. 1992. Target enzyme recognition by calmodulin: 2.4A structure of a calmodulin–peptide complex. *Science 257*:1251–1255.

Meador WE, Means AR, Quiocho FA. 1993. Modulation of calmodulin plasticity in molecular recognition on the basis of X-ray structures. *Science 262*:1718–1721.

Ohki S-Y, Ikura M, Zhang M. 1997. Identification of Mg^{2+}-binding sites and the role of Mg^{2+} on target recognition by calmodulin. *Biochemistry 36*:4309–4316.

Olwin BR, Storm DT. 1985. Calcium binding to complexes of calmodulin and calmodulin binding proteins. *Biochemistry 24*:8081–8086.

Peersen PB, Madsen TS, Falke JJ. 1997. Intermolecular tuning of calmodulin by target peptides and proteins: Differential effects on Ca^{2+} binding and implications for kinase activation. *Protein Sci 6*:794–807.

Persechini A, Gansz KJ, Paresi RJ. 1996. A role in enzyme activation for the N-terminal leader sequence in calmodulin. *J Biol Chem 271*:19279–19282.

Smith VL, Doyle, KE, Maune, JF, Munjaal RP, Beckingham K. 1987. Structure and sequence of the *Drosophila-melanogaster* calmodulin gene. *J Mol Biol 196*:471–485.

Török K, Lane AN, Martin SR, Janot J-M, Bayley PM. 1992. Effects of calcium binding in the internal dynamic properties of bovine brain calmodulin, studied by NMR and optical spectroscopy. *Biochemistry 31*:3452–3462.

Tsai M-D, Drakenberg T, Thulin E, Forsén S. 1987. Is the binding of magnesium(II) to calmodulin significant—An investigation by magnesium-25 nuclear-magnetic-resonance. *Biochemistry 26*:3635–3643.

Tsalkova TN, Privalov PL. 1985. Thermodynamic study of domain organization in troponin C and calmodulin. *J Mol Biol 181*:533–544.

van Gunsteren WF, Billeter SR, Eising AA, Huenenberger PH, Krueger P, Mark AE, Scott WRP, Tironi IG. 1996. Biomolecular simulation: The GROMOS96 manual and user guide. Zürich: vdf Hochschulverlag AG.

Vriend G. 1990. WHAT IF: A molecular modelling and drug design program. *J Mol Graph 8*:52–55.

Walsh M, Stevens FC, Kuznicki J, Drabikowski W. 1977. Characterization of tryptic fragments obtained from bovine brain protein modulator of cyclic nucleotide phosphodiesterase. *J Biol Chem 252*:7440–7443.

Yaswen P, Smoll A, Hosoda J, Parry G, Stampfer MR. 1992. Protein product of a human intronless calmodulin-like gene shows tissue-specific expression and reduced abundance in transformed-cells. *Cell Growth Diff 3*:333–345.

Yazawa M, Vorherr T, James P, Carafoli E, Yagi K. 1992. Binding of calcium by calmodulin: Influence of the calmodulin binding domain of the plasma membrane calcium pump. *Biochemistry 31*:3171–3176.